

LA-UR 98-4082 to appear in the Proceedings of the 1st International Conference on Quasiclassical Methods in Superconductivity, eds. D. Rainer and J.A. Sauls, Verditz, Austria (1998)

Electronic Transport in Unconventional Superconductors

Matthias J. Graf

Center for Materials Science, Los Alamos National Laboratory,
Los Alamos, New Mexico 87545, USA

Abstract. We investigate the electronic transport coefficients in unconventional superconductors at low temperatures, where charge and heat transport are dominated by electron scattering from random lattice defects. We discuss the features of the pairing symmetry, Fermi surface, and excitation spectrum which are reflected in the low temperature heat transport. For temperatures $k_B T \lesssim \gamma \ll \Delta_0$, where γ is the bandwidth of impurity induced Andreev states, certain eigenvalues become *universal*, i.e., independent of the impurity concentration and phase shift. Deep in the superconducting phase ($k_B T \lesssim \gamma$) the Wiedemann-Franz law, with Sommerfeld's value of the Lorenz number, is recovered. We compare our results for theoretical models of unconventional superconductivity in high- T_c and heavy fermion superconductors with experiment. Our findings show that impurities are a sensitive probe of the low-energy excitation spectrum, and that the zero-temperature limit of the transport coefficients provides an important test of the order parameter symmetry.¹

1 Introduction

Heat and charge transport in metals provides valuable information on the spectrum of charge carriers and phonons, as well as the scattering of the carriers by defects and impurities. In a normal metal at low temperatures the contribution of the phonons to the electrical and thermal conductivities becomes negligible compared to the electronic part. When the temperature is further reduced the electronic transport is dominated by scattering of electrons from lattice defects. Eventually the electrical conductivity approaches a constant, $\sigma(T) \propto \text{constant}$, while the thermal conductivity becomes linear in temperature, $\kappa(T) \propto T$. Both transport coefficients are related by the Wiedemann-Franz (WF) law $\kappa/(\sigma T) = L_S$, with Sommerfeld's result for the Lorenz number $L_S = \frac{\pi^2}{3}(k_B/e)^2$. Inelastic scattering leads to violations of the WF law and to significant deviations from L_S .

¹ This work was done in collaboration with S.-K. Yip, J. A. Sauls, and D. Rainer.

This picture is dramatically altered upon entering the superconducting phase with the formation of a pair condensate and the opening of a gap in the excitation spectrum. The excitation gap in conventional (*s*-wave) superconductors destroys the WF law. This effect has been known since the early days of the BCS (Bardeen, Cooper & Schrieffer 1957) theory of superconductivity from the work of Mattis and Bardeen (1958) on the electrical conductivity, and from the analysis of Geilikman (1958) of the heat transport.

In this article we investigate the behavior of the heat current for an unconventional superconductor, *i.e.*, for an order parameter with reduced symmetry for which gapless excitations exist even at zero temperature. Such superconducting states have been argued to exist both in the cuprates and heavy fermion superconductors. [For reviews on the heavy fermion system UPt₃ see, e.g., Sauls (1994a), and Heffner & Norman (1996), and on the cuprates, e.g., Pines (1994a), and Scalapino (1995)]. The leading pairing candidate for a tetragonal crystal structure (D_{4h}) in the cuprates is the B_{1g} state, a spin-singlet state with lines of nodes at the Fermi positions $p_{fx} = \pm p_{fy}$. The most promising candidates in the heavy fermion system UPt₃ are the two-dimensional orbital representations coupled to a symmetry breaking field. For UPt₃, which has a hexagonal crystal structure (D_{6h}), phase diagram studies (Bruls *et al.* 1990, Adenwalla *et al.* 1990), and transport measurements (Shivaram *et al.* 1986, Müller *et al.* 1987, Broholm *et al.* 1990, Signore *et al.* 1995) lead to either an even-parity, spin singlet E_{1g} state, or an odd-parity, spin triplet E_{2u} pairing state. In both cases the order parameter vanishes at the Fermi surface on a line in the basal plane, $p_{fz} = 0$, and at points at the poles, $p_{fx} = p_{fy} = 0$. Other models studied in the Ginzburg-Landau regime include the one-dimensional orbital, spin triplet model with weak spin-orbit coupling by Machida & Ozaki (1991) and Ohmi & Machida (1993), the accidental degeneracy AB-model with two unrelated one-dimensional orbital representations by Chen & Garg (1993, 1994), and the accidental degeneracy AE-model by Zhitomirsky & Ueda (1996).

It is known that in a *clean* superconductor with an order parameter that vanishes along a line on the Fermi surface the low-energy density of states is linear in the excitation energy, $N(\epsilon) \sim N_f \epsilon / \Delta_0$ for $\epsilon < \Delta_0$, which leads at low temperatures to a power law behavior in transport properties as a function of temperature for $T \ll T_c$ (Coffey *et al.* 1985, Pethick & Pines 1986, Barash *et al.* 1996). Gor'kov & Kalugin (1985) and later Choi & Muzikar (1988) showed that this spectrum is altered by a random distribution of impurities. A new low energy scale, γ , emerges below which the density of states is approximately constant and non-zero at zero energy. The energy scale γ is interpreted as the bandwidth of quasiparticle states bound to impurities (Shiba 1968, Rusinov 1969, Buchholtz & Zwicknagl 1981, Preosti *et al.* 1994, Balatsky *et al.* 1995). These impurity-induced states develop below the superconducting transition. They are formed by the constructive interference of particle- and hole-like excitations that undergo Andreev scattering from the anisotropy of the order parameter in momentum space. For an order parameter with a line of nodes that is required by symmetry, the bandwidth and density of Andreev states at zero energy are finite for any

finite concentration of impurities, $n_i \neq 0$. Both γ and $N(0)$ depend on the impurity concentration n_i and the scattering phase shift δ_0 . Thus, γ defines a crossover energy scale or crossover temperature T^* , below which the transport properties are dominated by the Andreev states. For excitation energies above γ the transport properties are determined primarily by the scattering of continuum excitations.

We study in detail the low temperature behavior of the thermal conductivity tensor for unconventional superconductors with line and point nodes in the order parameter. One of the issues we address is the universality of the electrical and thermal conductivities at low temperature. We show that the components of the thermal conductivity tensor that depend on quasiparticles near the line nodes are determined by the same scattering rate as the electrical conductivity and are universal in the limit $T \rightarrow 0$. Furthermore, we show that the WF law is recovered in the limit $T \ll T^*$, independent of the universality of the transport coefficients. However, a significant temperature dependence of the Lorenz ratio occurs over the temperature range, $T^* \lesssim T < T_c$, even for elastic scattering. The universal eigenvalues for κ and σ result from the cancellation between two factors: (i) the density of Andreev states, which is proportional to $N(\epsilon \rightarrow 0) \sim N_f \gamma / \Delta_0$, and (ii) the reduction of phase space for scattering of gapless excitations, which is proportional to $\tau(\epsilon \rightarrow 0) \sim \hbar / \gamma$. This leads to estimates for the electrical conductivity, $\sigma(T) \sim N(\epsilon) v_f^2 \tau(\epsilon) \sim N_f v_f^2 (\hbar / \Delta_0)$, and the thermal conductivity, $\kappa(T) \sim N(\epsilon) k_B^2 T v_f^2 \tau(\epsilon) \sim N_f v_f^2 k_B^2 T (\hbar / \Delta_0)$, which are independent of the defect density or scattering phase shift. Perhaps the most surprising result is that the ratio of the thermal and electrical conductivity gives the Sommerfeld value for the Lorenz ratio, $\kappa / \sigma T \simeq L_S = \frac{\pi^2}{3} (k_B / e)^2$. Thus, the differences in the coherence factors that determine the conductivity tensors, κ and σ , do *not* affect the Lorenz ratio $L(T) = \kappa / \sigma T$ for $T \ll T^*$ and $\hbar \omega \ll \gamma$. This discovery was made independently by Sun & Maki (1995) for a two-dimensional $d_{x^2-y^2}$ superconductor. For temperatures above the crossover region, $T > T^*$, the Lorenz ratio deviates significantly from the Sommerfeld value. The WF law breaks down due to the energy dependence of the scattering lifetime in the superconducting state, although scattering of electrons from impurities is purely elastic.

The rest of this article is organized as follows. First we introduce the linear response theory for charge and heat currents in unconventional superconductors. Then we discuss in general the conditions necessary for observing the Wiedemann-Franz law deep in the superconducting state. Next, several order parameter models are introduced and the low-temperature behavior of the corresponding electrical and thermal conductivities are discussed. Finally, we compute the thermal conductivities in the superconducting phase and compare our results with recent experimental measurements in UPt₃ and Zn doped YBa₂Cu₃O_{6.9} single crystals.

2 Electrical and Thermal Conductivities

We consider a superconductor with anisotropic singlet pairing or unitary triplet pairing and discuss the electrical and thermal conductivities in the long wavelength limit $q \rightarrow 0$, and at temperatures $T \rightarrow 0$. For simplicity we assume isotropic impurity scattering, which we treat self-consistently to leading order in $1/k_f \xi_0$. In this case the first order corrections to the current response functions of the impurity self-energy, $\delta\hat{\sigma}_{imp}$, and the order parameter, $\delta\hat{\Delta}$, vanish for all pairing states listed in Table 1. Self-energy corrections corresponding to the excitation of collective modes of the order parameter, $\delta\hat{\Delta}$, also vanish in the limit $q \rightarrow 0$ (Hirschfeld *et al.* 1989, Yip *et al.* 1992). The self-energy corrections are also called ‘vertex corrections’ in the Green function formalism of the Kubo response function (Rickayzen 1976). If vertex corrections do not contribute, the response functions for the electrical and thermal conductivities depend only on the equilibrium propagators and self-energies, and the external perturbations. A detailed derivation and justification of the linear response in the quasiclassical formulation of a Fermi liquid has been given earlier by several authors and is repeated in brief in the Appendix. Hence we simply present the response functions and start with the discussion of our results for various order parameter models.

For spin singlet states the electrical conductivity is given by

$$\begin{aligned} \text{Re } \sigma_{ij}(\omega, T) &= \frac{e^2 N_f \hbar}{\pi \omega} \int d\epsilon \int d\mathbf{p}_f v_{f,i} v_{f,j} [f(\epsilon_-) - f(\epsilon_+)] \\ &\times \text{Re} \left\{ M^R(\mathbf{p}_f; \epsilon, \omega) \left(g_0^R(\mathbf{p}_f; \epsilon_-) g_0^R(\mathbf{p}_f; \epsilon_+) + \underline{f}_0^R(\mathbf{p}_f; \epsilon_-) f_0^R(\mathbf{p}_f; \epsilon_+) + \pi^2 \right) \right. \\ &\left. - M^a(\mathbf{p}_f; \epsilon, \omega) \left(g_0^A(\mathbf{p}_f; \epsilon_-) g_0^R(\mathbf{p}_f; \epsilon_+) + \underline{f}_0^A(\mathbf{p}_f; \epsilon_-) f_0^R(\mathbf{p}_f; \epsilon_+) + \pi^2 \right) \right\}, \quad (1) \end{aligned}$$

where $\epsilon_{\pm} = \epsilon \pm \hbar\omega/2$, and $f(\epsilon)$ is the Fermi-Dirac distribution function, and $\int d\mathbf{p}_f \dots$ is a normalized Fermi surface integral. For triplet pairing the spin scalar product is replaced by its corresponding spin vector product, $\underline{f}_0 f_0 \rightarrow \underline{\mathbf{f}}_0 \cdot \mathbf{f}_0$. The *retarded* (R) and *anomalous* (a) auxiliary functions M^X are defined as (for more details see the Appendix),

$$M^X(\mathbf{p}_f; \epsilon, \omega) = \frac{C_+^X(\mathbf{p}_f; \epsilon, \omega)}{\pi^2 C_+^X(\mathbf{p}_f; \epsilon, \omega)^2 + D_-^X(\epsilon, \omega)^2} \quad \text{for } X \in \{R, a\}. \quad (2)$$

The result for $\sigma_{ij}(\omega, T)$ was obtained earlier for electron-phonon and impurity scattering in conventional superconductors in the strong coupling limit by Lee *et al.* (1989) and for the in-plane conductivity of layered weak-coupling superconductors by Graf *et al.* (1995). The conductivity formula reduces for a dirty s -wave superconductor to the well-known result of Mattis and Bardeen (1958).

In contrast to σ_{ij} , the thermal conductivity for a spin singlet state is determined solely by the anomalous part of the response function,

$$\begin{aligned} \kappa_{ij}(T) = & \frac{N_f}{\pi k_B T} \int d\epsilon \int d\mathbf{p}_f v_{f,i} v_{f,j} \epsilon^2 \frac{\partial f(\epsilon)}{\partial \epsilon} \\ & \times M^a(\mathbf{p}_f; \epsilon, 0) \left(g_0^A(\mathbf{p}_f; \epsilon) g_0^R(\mathbf{p}_f; \epsilon) - \underline{f}_0^A(\mathbf{p}_f; \epsilon) f_0^R(\mathbf{p}_f; \epsilon) + \pi^2 \right). \end{aligned} \quad (3)$$

The retarded and advanced contributions dropped out after applying the normalization condition. Physically, this means that the deviation of the quasiparticle distribution function due to a thermal gradient determines the heat current; changes in the quasiparticle and Cooper pair spectrum do not. Equation (3), combined with the equilibrium propagators, impurity self-energy and order parameter, is the basic result for the electronic contribution to the thermal conductivity tensor. It can be shown that κ_{ij} in equation (3) reduces to the same expression for the thermal conductivity as reported earlier by Schmitt-Rink *et al.* (1986), Hirschfeld *et al.* (1986, 1988), and Fledderjohann & Hirschfeld (1995), except that these authors do not include the $D^{\underline{a}}$ term from the impurity self-energy. The D^X terms are only significant at low temperatures, where they can help to distinguish between magnetic and nonmagnetic impurities, and vanish in both Born and unitarity limits.

2.1 The Wiedemann-Franz law

In the limit $T \rightarrow 0$ and $\omega \rightarrow 0$ the occupation factors $f(\epsilon - \frac{\hbar\omega}{2}) - f(\epsilon + \frac{\hbar\omega}{2})$ and $\partial f(\epsilon)/\partial \epsilon$ confine the ϵ -integrals in (1) and (3) to a small ϵ -region of order $k_B T$ or $\hbar\omega$. Assuming the existence of an energy scale $\epsilon^* \gg k_B T$, on which the propagators and self-energies vary, we can set $\epsilon = 0$ in the slowly varying parts of the integrands. Using the normalization condition, $g_0^R(\mathbf{p}_f)^2 - \underline{f}_0^R(\mathbf{p}_f) f_0^R(\mathbf{p}_f) = -\pi^2$, in addition to the general symmetry relations for the Green functions, we obtain for the conductivities

$$\text{Re } \sigma_{ij}(\omega \rightarrow 0, T \rightarrow 0) = \frac{2e^2 N_f \hbar}{\pi} \int d\epsilon \left(-\frac{\partial f(\epsilon)}{\partial \epsilon} \right) \int d\mathbf{p}_f v_{f,i} v_{f,j} \frac{g_0^R(\mathbf{p}_f)^2}{\pi^2 C_+^R(\mathbf{p}_f)}, \quad (4)$$

and

$$\kappa_{ij}(T \rightarrow 0) = \frac{2N_f \hbar}{\pi k_B T} \int d\epsilon \epsilon^2 \left(-\frac{\partial f(\epsilon)}{\partial \epsilon} \right) \int d\mathbf{p}_f v_{f,i} v_{f,j} \frac{g_0^R(\mathbf{p}_f)^2}{\pi^2 C_+^R(\mathbf{p}_f)}. \quad (5)$$

It is useful to write our final results in terms of a mean Fermi velocity and an *effective* transport scattering time τ_{ij} , which incorporates all of the coherence effects of superconductivity at $T \rightarrow 0$.

The energy integrals are standard, so the conductivities for a system with D dimensions reduce to

$$\text{Re } \sigma_{ij}(\omega \rightarrow 0, T \rightarrow 0) = e^2 \frac{2}{D} N_f v_{f,i} \tau_{ij} v_{f,j}, \quad (6)$$

$$\kappa_{ij}(T \rightarrow 0) = \frac{\pi^2 k_B^2}{3} T \frac{2}{D} N_f v_{f,i} \tau_{ij} v_{f,j}, \quad (7)$$

where $v_{f,i}^2 = \int d\mathbf{p}_f \mathbf{v}_{f,i}(\mathbf{p}_f)^2$, and the effective transport time is defined by the tensor

$$\tau_{ij} = -\frac{D\hbar}{2v_{f,i}v_{f,j}} \int d\mathbf{p}_f \frac{v_{f,i}(\mathbf{p}_f)v_{f,j}(\mathbf{p}_f) \tilde{\epsilon}^R(0)^2}{\left(|\Delta(\mathbf{p}_f)|^2 - \tilde{\epsilon}^R(0)^2\right)^{3/2}}. \quad (8)$$

Here $\tilde{\epsilon}^R(\epsilon)$ is the impurity renormalized quasiparticle excitation spectrum.

For an isotropic normal metal one has $\tilde{\epsilon}^R(0) = i\hbar/2\tau$, where τ is the quasiparticle lifetime due to impurity scattering in the normal state. The transport lifetime in the normal state reduces to τ for isotropic impurity scattering, i.e., $\tau_{ij} = \tau\delta_{ij}$. Note that expression (8) is applicable to the normal state because the key assumption in deriving (6) and (7) was that T is small compared with ϵ^* , where ϵ^* is the energy on which the propagators and self-energies vary. Thus, for the normal state $\epsilon^* \sim E_f$, while for the superconducting state $\epsilon^* \sim \gamma$, where γ is the impurity bandwidth of Andreev states, defined by the transcendental equation

$$1 = \frac{n_i}{\pi N_f} \frac{\langle 1/\sqrt{|\Delta(\mathbf{p}_f)|^2 + \gamma^2} \rangle}{\cot^2 \delta_0 + \langle \gamma/\sqrt{|\Delta(\mathbf{p}_f)|^2 + \gamma^2} \rangle^2}, \quad (9)$$

with the Fermi surface average $\langle \dots \rangle$, the scattering phase shift δ_0 , and the impurity concentration n_i .

In some respect the band of impurity states forms a new low-temperature metallic state deep in the superconducting phase. This analogy becomes more transparent when we calculate the temperature corrections to the transport coefficients, using a Sommerfeld expansion. However, the ‘metallic’ band of impurity states has other properties that differ significantly from those of conventional metals. The special features of the impurity induced metallic band reflect the reduced dimensionality of phase space for scattering and the energy dependence of the particle-hole coherence factors. Both features combined lead to (i) the universality of the transport coefficients at $T \rightarrow 0$ for excitation gaps with line nodes or quadratic point nodes, and (ii) the temperature dependence of the Lorenz ratio for elastic scattering at $T^* < T < T_c$.

We emphasize that (6) and (7) hold for gapless superconductors in which the leading contribution to the transport current is that from quasiparticle excitations with energies $T \lesssim T^* \ll T_c$. For superconductors with a gap at the Fermi surface the number of quasiparticle excitations is of an activated type at low temperatures, $\sim \exp(-\Delta_0/T)$, and thus the transport coefficients cannot be described by equations (6) and (7), with the consequence that the Wiedemann-Franz law is strongly violated below T_c .

2.2 Order parameter models

In our analysis we take a very simple approach. Instead of examining the effects of a multi-sheet Fermi surface on the heat and charge current, we model the

excitation spectrum by an excitation gap that opens at line and point nodes on the Fermi surface, and by the Fermi surface properties in the vicinity of the nodes (*i.e.* the Fermi velocities, \mathbf{v}_f , and the density of states, N_f , near the nodes). The low-temperature behavior of the transport coefficients probes these ‘lower-dimensional’ regions of the Fermi surface, $\epsilon \ll \Delta_0 \ll E_f$, where the excitation gap vanishes, and is less sensitive to the overall geometry of the Fermi surface. It is therefore admissible to parametrize the nodal regions of the gap with a minimal set of nodal parameters. The advantage of this approach is that we can quantitatively determine the phase space contributing to the low-temperature transport coefficients and then examine in more detail the effects of impurity scattering and order parameter symmetry on the heat current, without having to know the overall shape of the Fermi surface or basis functions.

We consider models for the order parameter belonging to several irreducible representations of the D_{6h} and D_{4h} symmetry groups, which are chosen because they represent the primary candidates for the pairing symmetry of the heavy fermion superconductor UPt₃ [for more details on the heat conduction at low temperatures for the various order parameter models see Graf *et al.* (1999)], and the high T_c superconductor YBa₂Cu₃O_{6.9}.² The singlet and triplet pairing states, we consider, have the form

$$\text{(singlet)} \quad \Delta(\mathbf{p}_f) = \Delta_0(T) \mathcal{Y}_\Gamma(\mathbf{p}_f), \quad (10)$$

$$\text{(triplet)} \quad \mathbf{\Delta}(\mathbf{p}_f) = \Delta_0(T) \mathcal{Y}_\Gamma(\mathbf{p}_f) \hat{\mathbf{d}}, \quad (11)$$

where $\hat{\mathbf{d}}$ is the quantization axis along which the pairs have zero spin projection.³

The basis functions \mathcal{Y}_Γ listed in Table 1 have nodes in the order parameter and excitation gap that are dictated by symmetry. We model the different nodal regions of the gap by a set of parameters, $\{\mu_i\}$ that determine the variation of the gap near the nodes (Graf *et al.* 1996a). Consider the E-rep models shown in Fig. 1. In the vicinity of the equatorial line node ($p_{fz} = 0$), $|\Delta(\theta)| \sim \mu_{\text{line}} \Delta_0 |\Theta|$, while near the poles ($p_{fx} = p_{fy} = 0$), $|\Delta(\theta)| \sim \mu_{\text{point}} \Delta_0 |\Theta|^n$, where the internal phase winding number is $n = 1$ for E_{1g} and $n = 2$ for E_{2u} .⁴

2.3 Universal limits and low temperature corrections

For simplicity we restrict our discussion of the universal limits and low- T corrections to the E-rep models proposed for UPt₃, and list the asymptotic values for

² For detailed discussions of the possible pairing models in UPt₃ and high T_c superconductors see the reviews on UPt₃ by Sauls (1994a) and Heffner & Norman (1996), and on the cuprates by Pines (1994a) and Scalapino (1995).

³ In this analysis spin has no effect on the transport coefficients beyond the connection between the direction of the spin quantization axis and the nodal structure of the odd-parity, triplet state basis functions.

⁴ The parameters μ_{line} and μ_{point} define the slope or curvature of the gap near a nodal line or point in a spherical coordinate system that is obtained by mapping an ellipsoidal Fermi surface onto a sphere.

Table 1. Symmetry groups, irreducible representations, and the standard basis functions of the low temperature phase of several pairing models.

| Group | Γ | \mathcal{Y}_Γ | point nodes | line nodes |
|-----------------|--|--|----------------------|---|
| D _{4h} | B _{1g} | $k_x^2 - k_y^2$ | – | $\varphi_n = (2n + 1) \frac{\pi}{4}, n = 0, \dots, 3$ |
| D _{6h} | E _{1g} | $k_z (k_x + i k_y)$ | $\vartheta = 0, \pi$ | $\vartheta = \frac{\pi}{2}$ |
| D _{6h} | E _{2u} | $\hat{\mathbf{c}} k_z (k_x + i k_y)^2$ | $\vartheta = 0, \pi$ | $\vartheta = \frac{\pi}{2}$ |
| D _{6h} | B _{1u} | $\hat{\mathbf{c}} \text{Im} (k_x + i k_y)^3$ | $\vartheta = 0, \pi$ | $\varphi_n = n \frac{\pi}{3}, n = 0, \dots, 5$ |
| D _{6h} | A _{2u} \oplus i B _{1u} | $\hat{\mathbf{c}} [A k_z \text{Im} (k_x + i k_y)^6 + i B \text{Im} (k_x + i k_y)^3]$ | $\vartheta = 0, \pi$ | $\varphi_n = n \frac{\pi}{3}, n = 0, \dots, 5$ |
| D _{6h} | A _{1g} \oplus i E _{1g} | $A (2k_z^2 - k_x^2 - k_y^2) + i E k_y k_z]$ | cross-nodes: | $\vartheta = \cos^{-1} \frac{\pm 1}{\sqrt{3}}$ $\wedge \varphi = 0, \pi$ |

the other pairing models in Table 2. For a uniaxial, unconventional superconductor with an ellipsoidal Fermi surface a Sommerfeld expansion of the charge and heat conductivity tensors gives

$$\begin{aligned} \sigma_i(T) &\simeq \alpha_{\sigma,i} + \beta_{\sigma,i} T^2, \\ \kappa_i(T)/T &\simeq \alpha_{\kappa,i} + \beta_{\kappa,i} T^2, \end{aligned} \quad \text{for } i = a, b, c. \quad (12)$$

In the strong scattering limit the parameters α_b and β_b are related to the microscopic model parameters by

$$\alpha_{\kappa,b} \simeq \frac{v_{f,b}^2}{3} \gamma_S \tau_\Delta, \quad \frac{\beta_{\kappa,b}}{\alpha_{\kappa,b}} \simeq \frac{7\pi^2 k_B^2}{60 \gamma^2}, \quad (13)$$

$$\alpha_{\sigma,b} \simeq \frac{3e^2}{\pi^2 k_B^2} \alpha_{\kappa,b}, \quad \frac{\beta_{\sigma,b}}{\alpha_{\sigma,b}} \simeq \frac{5}{7} \frac{\beta_{\kappa,b}}{\alpha_{\kappa,b}}. \quad (14)$$

Here $\gamma_S = \frac{2}{3} \pi^2 k_B^2 N_f$ is the normal-state Sommerfeld coefficient, and the *effective* transport scattering time is defined by $\tau_a = \tau_b = \tau_\Delta$, where

$$\tau_\Delta = 3\hbar / (4\mu_{\text{line}} \Delta_0(0)). \quad (15)$$

For heat flow along the *c*-axis the coefficients depend sensitively on the internal phase winding number, n , of the order parameter around the point nodes,

$$\alpha_{\kappa,c} \simeq \frac{v_{f,c}^2}{3} \gamma_S \frac{3\hbar}{4\mu_{\text{point}} \Delta_0(0)} \times \begin{cases} 2\gamma / \mu_{\text{point}} \Delta_0(0), & (\text{E}_{1g}) \\ 1, & (\text{E}_{2u}) \end{cases}, \quad (16)$$

$$\alpha_{\sigma,c} \simeq \frac{3e^2}{\pi^2 k_B^2} \alpha_{\kappa,c}, \quad (17)$$

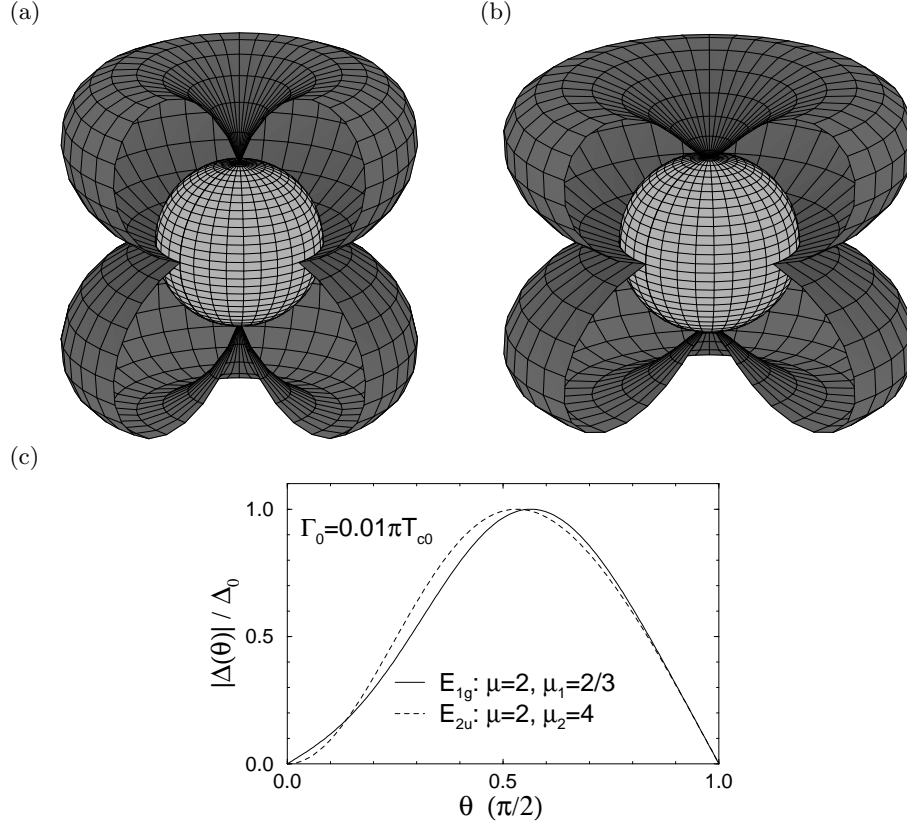


Fig. 1. The excitation gap (exaggerated) at the Fermi surface (sphere) for E_{1g} (a) and E_{2u} (b) order parameters showing the line node in the basal plane and the linear and quadratic point nodes at the poles. Panel (c) shows the normalized excitation gap at $T = 0$ for both states as a function of the polar angle Θ . The parameters correspond to those that fit the low temperature thermal conductivity data shown in Fig. 4.

$$\frac{\beta_{\kappa,c}}{\alpha_{\kappa,c}} \simeq \frac{7\pi^2 k_B^2}{120\gamma^2} \times \begin{cases} 5, (E_{1g}) \\ 2, (E_{2u}) \end{cases}, \quad \frac{\beta_{\sigma,c}}{\alpha_{\sigma,c}} \simeq \frac{1}{7} \frac{\beta_{\kappa,b}}{\alpha_{\kappa,b}} \times \begin{cases} 3, (E_{1g}) \\ 5, (E_{2u}) \end{cases}. \quad (18)$$

One important result is that at low temperatures the *basal plane* transport measurements cannot distinguish between the two pairing models, whereas *c*-axis transport coefficients are sensitive to the symmetry of the pairing state. Small variations in the concentration of defects may be used to probe the symmetry of the pairing state. This is evident in the asymptotic slope of the thermal conductivity $\alpha_{\kappa,c} = \lim_{T \rightarrow 0} \kappa_c/T$, which is universal for the E_{2u} state, but depends on the impurity concentration (n_i) for the E_{1g} state. Furthermore, in the unitarity scattering limit $\gamma^2 \propto n_i$; thus, the coefficient of the T^3 term scales with the impurity concentration as $\beta_c \sim 1/n_i$ for the E_{2u} state and $\beta_c \sim 1/\sqrt{n_i}$ for the

E_{1g} state.

The leading order finite temperature corrections to the Wiedemann-Franz ratio become

$$L(T) = \frac{\kappa_b(T)}{T \operatorname{Re} \sigma_b(T, \omega \rightarrow 0)} \simeq L_S \left(1 + \left[\frac{\beta_\kappa}{\alpha_\kappa} - \frac{\beta_\sigma}{\alpha_\sigma} \right] T^2 \right) \simeq L_S \left(1 + \frac{\pi^2 k_B^2 T^2}{30 \gamma^2} \right), \quad (19)$$

which increases with temperature for $T \lesssim T^* \sim \gamma/k_B$. This behavior arises from two sources: (i) the residual density of states at $\epsilon = 0$, $N(0) \sim N_f(\gamma/\Delta_0)$, and (ii) the difference in the coherence factors between thermal and electrical conduction. Note that for weak scattering, or very clean materials, the very low-temperature regime $T < T^*$ may be difficult to achieve in practice.

The asymptotic limits for the order parameter models listed in Table 1 are summarized in Table 2. Note the universal result for the in-plane thermal conductivity of the $d_{x^2-y^2}$ model for the high T_c superconductors. We omit the asymptotic value of the out-of-plane conductivity in the cuprates because it strongly depends on the model for the interlayer transport (*i.e.* coherent vs. incoherent propagation of quasiparticles).

Table 2. Asymptotic values of the thermal conductivity tensor κ/T at $T \rightarrow 0$.

| Pairing State | Rep (Group) | $\kappa_b(T) \left(\frac{1}{2} \gamma_S T v_{f,b}^2 \right)^{-1}$ | $\kappa_c(T) \left(\frac{1}{2} \gamma_S T v_{f,c}^2 \right)^{-1}$ |
|---------------|--------------------------------------|--|--|
| $d_{x^2-y^2}$ | B_{1g} (D_{4h}) | $2/(\pi\mu\Delta_0)$ | — |
| hybrid-I | E_{1g} (D_{6h}) | $1/(2\mu\Delta_0)$ | $\gamma/(\mu_1^2\Delta_0^2)$ |
| hybrid-II | E_{2u} (D_{6h}) | $1/(2\mu\Delta_0)$ | $1/(2\mu_2\Delta_0)$ |
| spin triplet | B_{1u} (D_{6h}) | $3/(2\mu\Delta_0)$ | $\sim \frac{1}{\mu_3\Delta_0} (\mu_3\Delta_0/\gamma)^{\frac{1}{3}}$ |
| AB-model | $A_{2u} \oplus iB_{1u}$ (D_{6h}) | $3/(2\mu\Delta_0)$ | $\sim \frac{(\mu_3\Delta_0/\gamma)^{\frac{1}{3}}}{\mu_3\Delta_0}$ for $\mu_3 \sim 1$ |
| AE-model | $A_{1g} \oplus iE_{1g}$ (D_{6h}) | $\frac{\sim \gamma^3}{(\mu_A\Delta_0^A)(\mu_E\Delta_0^E)^3}$ | $\frac{\sim \gamma}{(\mu_A\Delta_0^A)(\mu_E\Delta_0^E)}$ |

The low temperature anisotropy ratio $\kappa_c(T)/\kappa_b(T)$, suggested as a symmetry probe by Fledderjohann and Hirschfeld (1995), distinguishes between the different E-rep pairing models and is very sensitive to the impurity concentration, see Table 2. The experimentally observed anisotropy ratio in UPt₃ (Lussier *et al.* 1996) approaches the value

$$\lim_{T \rightarrow 0} \frac{\kappa_c(T)}{\kappa_b(T)} \approx 0.4 \frac{\kappa_c(T_c)}{\kappa_b(T_c)}. \quad (20)$$

Assuming scattering in the unitarity limit and a reasonable value for the scattering rate $\Gamma(T_c) = \hbar/2\tau(T_c) \approx 0.06 \dots 0.12 k_B T_c$, we can account for the data with both pairing states E_{1g} and E_{2u} by adjusting the nodal parameters at the poles. We also can account for the data within the AE-model of Zhitomirsky & Ueda (1996) by fitting the nodal parameters of the crossing line nodes (cross-nodes). States with cubic point nodes, *e.g.* the spin triplet model B_{1u} by Machida and coworkers (1991, 1993) and the accidental degeneracy AB-model $A_{2u} \oplus iB_{1u}$ by Chen & Garg (1993, 1994), have a much larger phase space contribution from the quasiparticles scattering from impurities near the nodes. Further experiments on UPt_3 with controlled studies for various impurity concentrations should distinguish between the E-rep and AE models as shown for the E-rep models in Fig. 2.

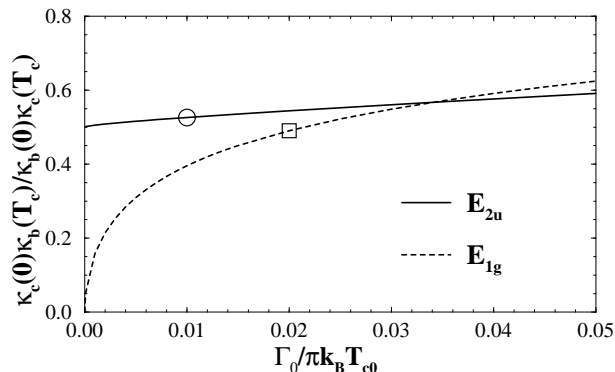


Fig. 2. Impurity dependence of the thermal conductivity ratio for an E_{1g} and E_{2u} order parameter. The symbols are the low-temperature fits of the impurity concentration for the UPt_3 single crystal measured by Lussier *et al.* (1996).

3 Numerical results

We explore the temperature dependence of the thermal conductivity for unconventional superconductors. Similar results were obtained earlier by several authors (see *e.g.* Schmitt-Rink *et al.* 1986, Hirschfeld *et al.* 1986, 1988, 1994, Monien *et al.* 1987, 1988, Arfi *et al.* 1988, 1989, Won *et al.* 1993, and Sun *et al.* 1995). What sets this work apart is the focus on the impurity induced band of Andreev states, and their influence on the low-temperature behavior of the heat current. Here we extend our analytic analysis with numerical calculations of the low- T behavior beyond the universal region. The numerical results are obtained by computing the equilibrium propagator, scattering self-energy, and

order parameter self-consistently. These results are then used to compute the transport coefficients.

3.1 Thermal conductivity in $\text{YBa}_2\text{Cu}_3\text{O}_{6.9}$

In Fig. 3 we plot for a $d_{x^2-y^2}$ -wave pairing state, $\Delta(\mathbf{p}_f) = \Delta_0 \cos 2\phi$, the thermal conductivity for several normalized scattering cross sections $\bar{\sigma} = \sin^2 \delta_0$, and normalized scattering rates $\alpha = \hbar/(2\pi k_B T_c \tau)$.⁵ A consequence of the universal limit is that the ratio

$$\lim_{T \rightarrow 0} \frac{\kappa(T) T_c}{\kappa(T_c) T} \simeq \frac{2\hbar}{\pi\tau\mu_{\text{line}}\Delta_0(0)} = \frac{4\Gamma}{\pi\mu_{\text{line}}\Delta_0(0)} \quad (21)$$

scales linearly with the scattering rate, Γ , and is independent of the scattering strength $\bar{\sigma}$. For $T \gtrsim T^*$ Arfi *et al.* (1989) have shown that $\kappa(T)/T \propto (1 - \bar{\sigma})\kappa(T_c)/T_c$ strongly depends on the scattering phase shift. This explains (i) the sudden drop of $[\kappa(T)T_c]/[\kappa(T_c)T]$ in Fig. 3(a) at ultra-low temperatures for weak scattering, where the universal limit is achieved only for $T \lesssim T^* \sim (2\mu_{\text{line}}\Delta_0/k_B) \exp(-\pi\mu_{\text{line}}\Delta_0/4\Gamma)$, and (ii) the scaling of the zero temperature intercept with α in Fig. 3(b). Below T^* the ratio κ/T approaches the universal limit. Weak scattering leads to an approximately linear temperature dependence over a large portion of the temperature range (Pethick *et al.* 1986, Barash *et al.* 1996). However, κ/T changes drastically in rather clean superconductors below the exponentially small crossover temperature, where it approaches its linear low-temperature asymptote.

Our calculations of the effects of the impurities on the low- T thermal conductivity assume a cylindrical Fermi surface and purely elastic scattering processes. These simplifications don't affect the low-temperature thermal conductivity since in this limit it is governed by the nodal points. However, we do not expect an accurate description of the experimental data at higher temperatures, $T \sim T_c$, where inelastic scattering is significant and excitations over the whole Fermi surface contribute to the transport properties.

Recently Taillefer *et al.* (1997) reported measurements of the heat conductivity in Zn doped $\text{YBa}_2(\text{Zn}_x\text{Cu}_{1-x})_3\text{O}_{6.9}$. The in-plane thermal conductivity was measured at temperatures as low as $T_c/1000$, and the predicted universal behavior of κ/T was observed for the first time. They found that the asymptotic value of κ/T is almost independent of the Zn concentration (0% – 3%), with $\lim_{T \rightarrow 0} \kappa/T \approx 18 \text{ mW/K}^2\text{m}$. They also found that phonons scattering off the crystal surfaces cannot be neglected in $\text{YBa}_2\text{Cu}_3\text{O}_{6.9}$ even at $T \sim T_c/1000$. The reported asymptotic value is somewhat larger than our previous estimate of $\kappa/T \approx 14 \text{ mW/K}^2\text{m}$ (Graf *et al.* 1996b) which is based on the expression

$$\lim_{T \rightarrow 0} \kappa/T = \frac{\pi^2}{3} \frac{k_B^2}{e^2} \frac{\omega_p^2 \tau_\Delta}{4\pi} = \frac{1}{2} \gamma_S v_f^2 \tau_\Delta, \quad (22)$$

⁵ Here we use simultaneously the notation of the dimensionless parameter α and $\Gamma = \hbar/2\tau$ for the scattering rate.

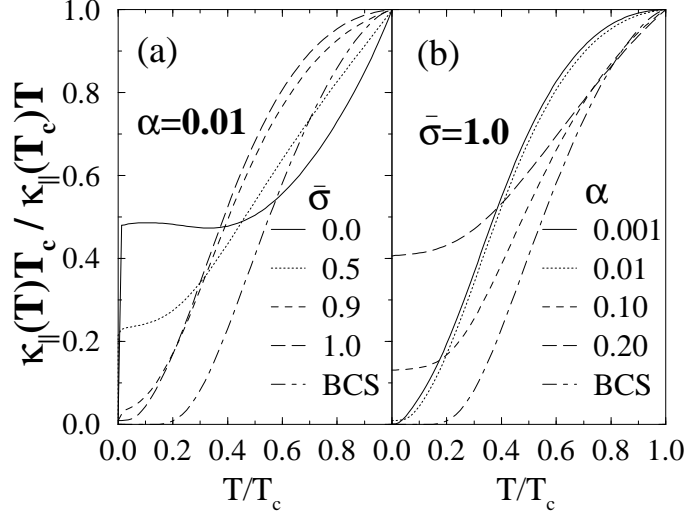


Fig. 3. Thermal conductivity of a 2D $d_{x^2-y^2}$ -wave superconductor. In panel (a): κ/T for different scattering cross sections, $\bar{\sigma}$, at a fixed scattering rate $\alpha = 0.01$. In panel (b): κ/T for different elastic scattering rates α in the unitarity limit ($\bar{\sigma} = 1.0$). The isotropic s -wave BCS result is shown for comparison.

with a Drude plasma frequency $\omega_p \approx 1.5$ eV, and $\tau_{\Delta} = \hbar/\pi\Delta_0(0)$, but is well within the uncertainties of the known material parameters. For example, if one uses specific heat measurements instead of the Drude plasma frequency, with typical values for the normal-state specific heat $C_{e1}/T = \gamma_S \approx 270 \pm 70$ J K⁻²m⁻³ (Junod *et al.* 1990), and the effective Fermi velocity near the nodal regions, $v_f \approx 110 \pm 20$ km/s, then we obtain $\kappa/T \approx 20$ mW/K²m.

3.2 Thermal conductivity in UPt₃

The inelastic scattering rate in UPt₃ is comparable to elastic scattering at T_c and dominated by electron-electron scattering in the normal state for 0.5 K $< T < 2$ K (Lussier *et al.* 1995). Elastic scattering is roughly isotropic (s -wave scattering). However, recent resistivity measurements by Kycia *et al.* (1998) show deviations of order 20% from isotropic scattering. In order to describe the temperature dependence of the thermal conductivity we model elastic scattering, Γ_0 , and inelastic scattering, Γ_{in} , by a phenomenological scattering rate $\Gamma(T) \equiv \hbar/2\tau(T) = \Gamma_0(1 + T^2/T_c^2)$, where we neglect the effects of anisotropic scattering. The inelastic scattering rate decreases below T_c even faster than T^2 because of the onset of superconductivity and the opening of a gap over most of the Fermi surface. We will neglect this reduction in $\Gamma(T)$, since we are mostly interested in the low-temperature regime, *e.g.* for temperatures $T \lesssim T_c/10$ the inelastic scattering rate is less than 1% and can safely be neglected. However, we do

not expect an accurate description of the experimental data in the temperature regime, $T_c/2 \lesssim T \leq T_c$, where inelastic scattering is not negligible.

Our analysis of the universal regime implies rather stringent restrictions on an equatorial line node

$$\lim_{T \rightarrow 0} \frac{\kappa_b(T)T_c}{\kappa_b(T_c)T} \simeq \frac{3}{2} \frac{\Gamma(T_c)}{\mu_{\text{line}}\Delta_0(0)}, \quad k_B T^* \simeq 0.2 \sqrt{\mu_{\text{line}}\Delta_0(0)} \Gamma_0. \quad (23)$$

The experimentally imposed constraints are consistent with a nodal parameter $\mu_{\text{line}} = 2$, an intercept of $[\kappa_b(T)T_c]/[\kappa_b(T_c)T] \lesssim 0.02$ at $T \rightarrow 0$, and a crossover temperature $T^* \lesssim T_c/12$ (Lussier *et al.* 1996, Huxley *et al.* 1996, Suderow *et al.* 1997). The elastic scattering rate Γ_0 is adjusted for a best fit to the low- T region for the basal plane thermal conductivity. For an E_{2u} pairing state a good fit is obtained for $\Gamma_0 = 0.01\pi T_{c0} \approx 0.03 T_c$, for which the theoretically computed intercept is

$$\lim_{T \rightarrow 0} \frac{\kappa_b(T)/T}{\kappa_b(T_c)/T_c} \approx 0.02. \quad (24)$$

This scattering rate fits the low-temperature part of the thermal conductivity in the superconducting state, but is smaller than that estimated from the normal-state transport data and de Haas-van Alphen data, $\Gamma_0 \approx 0.1 T_c - 0.2 T_c$, (Taillefer *et al.* 1987). Larger discrepancies were reported earlier by Lussier *et al.* (1995, 1996), and Fledderjohann *et al.* (1995). Finally, the nodal parameters defining the excitation gap near the point nodes are adjusted to fit the heat current along the c -axis, $\kappa_c(T)/T$ at $T \ll T_c$. These values are $\mu_1 = 2/3$ for the E_{1g} model and $\mu_2 = 4$ for the E_{2u} model.

A similar analysis for two of the other proposed pairing models for UPt_3 is shown in Fig. 5. It is in principal possible to fit the basal plane thermal conductivity, however, a fit for the heat current along the c -axis generally fails because of the large phase space contribution from the cubic point nodes and cross-nodes (crossing line nodes at the poles) for the B_{1u} and $A_{2u} \oplus iB_{1u}$ order parameters. This is the case for all order parameter models other than the E-rep models and the AE-model. Thus, the only models that are capable of explaining the existing data for the anisotropy and temperature dependence of the heat conductivity in UPt_3 are the 2D E-rep models and the AE-model.

The existing low-temperature data for the thermal conductivities of UPt_3 (Lussier *et al.* 1996) are equally well described by either an E_{1g} or E_{2u} or AE model. However one possibility to distinguish between these models is by studying the anisotropy ratio κ_c/κ_b in the low-temperature region for different scattering rates. The corresponding zero temperature limit for the E_{2u} (hybrid-II) state is universal, *i.e.* independent of impurity scattering for $\gamma \ll \Delta_0$. It depends only on the nodal (material) parameters through the ratio $\mu_{\text{line}}/\mu_{\text{point}}$. In contrast the anisotropy ratio for the E_{1g} state and AE pairing state depends sensitively on the scattering rate and scattering strength, see Fig. 6.

We summarize the quality of our fits of the thermal conductivity and the observable differences between the various models for the pairing state in UPt_3

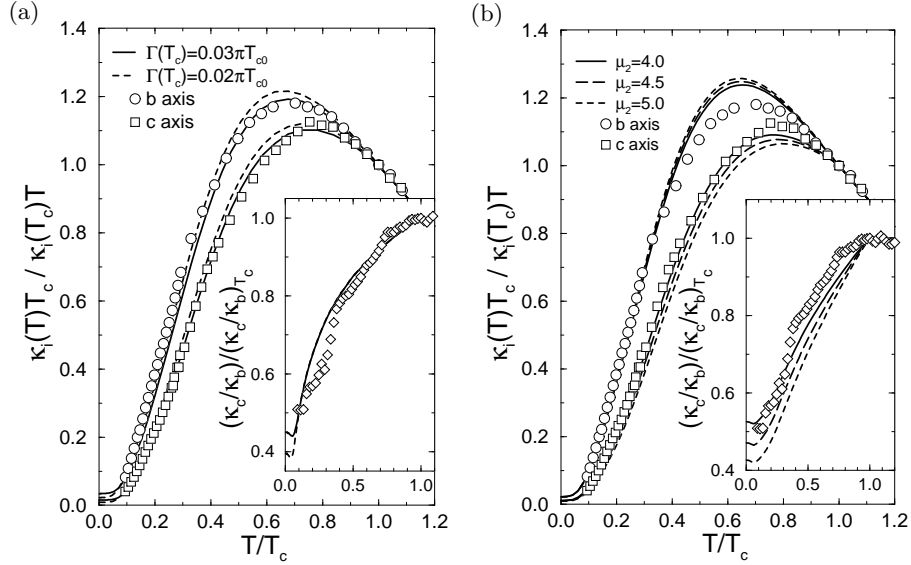


Fig. 4. Heat flow along the b and c axes in the unitarity limit. The experimental data (symbols) were taken from Lussier *et al.* (1996) and normalized to the values at $T_c \simeq 0.5$ K. The insets show the normalized anisotropy ratios. Panel (a): E_{1g} -state for two scattering rates $\Gamma(T_c)$. The slope parameters at the linear point nodes and at the line node were fixed to $\mu_1 = 2/3$ and $\mu_1 = 2.0$. Panel (b): E_{2u} -state with a scattering rate $\Gamma_0 = 0.01\pi k_B T_{c0}$ and different nodal parameters at the point nodes, $\mu_2 = 4.0, 4.5, 5.0$. The slope of the line node was fixed to $\mu_1 = 2.0$.

by plotting the anisotropy ratio $\mathcal{R}(T) = [\kappa_c(T)/\kappa_b(T)]/[\kappa_c(T_c)/\kappa_b(T_c)]$. Figure 7 shows that the ratio $\mathcal{R}(T)$ for the data of Lussier *et al.* (1996) is in agreement with the pairing states for the E_{1g} , E_{2u} , and AE models. The spin triplet model B_{1u} and the AB-model cannot account for the anisotropy at low temperatures, $\mathcal{R} < 1$. Independent measurements of the heat currents by Suderow *et al.* (1997) differ to some extent from those by Lussier *et al.* (1996), particularly in the ratio \mathcal{R} . This discrepancy is mainly due to differences in the heat current along the c -axis. This may be caused by crystal imperfections along the crystal c -axis, and needs further investigation.

4 Conclusion

At very low temperatures heat transport is dominated by elastic scattering of quasiparticles in lower dimensional regions of the Fermi surface in the vicinity of the nodes of the order parameter. As a result the low energy spectrum can be determined accurately without complete knowledge of the Fermi surface. The residual density of states at zero energy and zero temperature leads to a Wiedemann-Franz law for electronic transport deep in the superconduct-

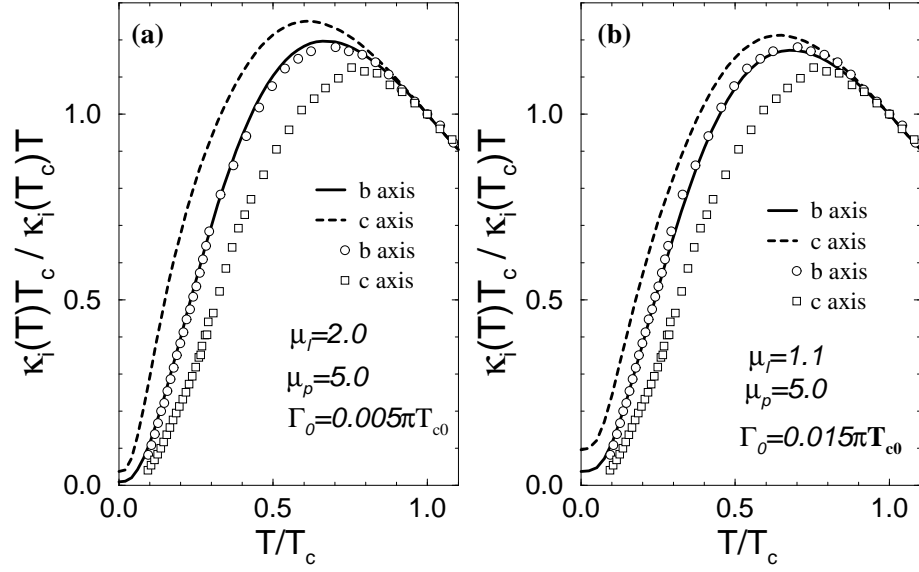


Fig. 5. The thermal conductivity for heat flow along the b and c axes in the resonant impurity scattering limit. The material parameters are the scattering rate, Γ_0 , and the nodal parameters, μ_i , at the point (p) and line (l) nodes. The theoretical results are compared with the experimental data (symbols) for UPt₃. Panel (a): fit for an odd-parity B_{1u} -state. Panel (b): fit for an accidentally degenerate $A_{2u} \oplus iB_{1u}$ -state.

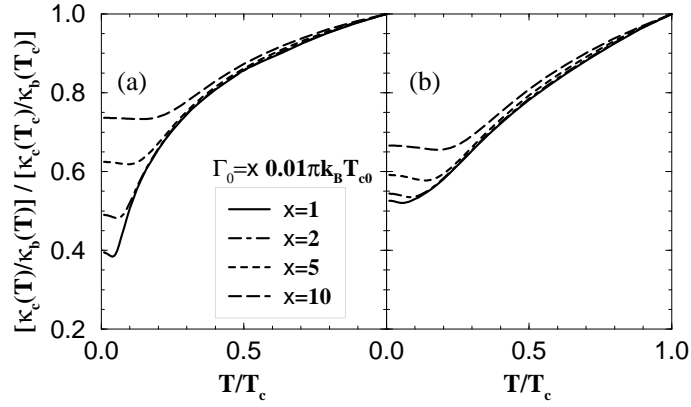


Fig. 6. Thermal conductivity ratio for a set of impurity scattering rates Γ_0 and a fixed $\Gamma_{\text{in}} = 0.01 \pi k_B T_{c0} (T/T_c)^2$ for an E_{1g} (a) and E_{2u} (b) pairing state.

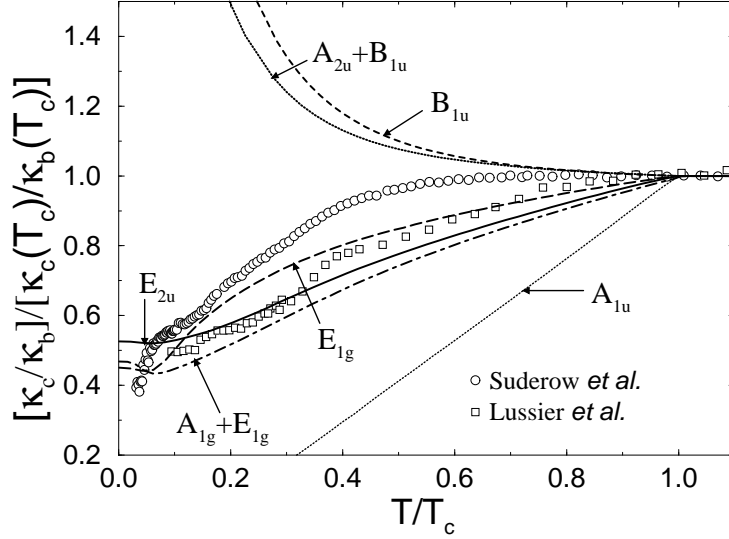


Fig. 7. The anisotropy ratio of the thermal conductivities for various ‘best fit’ pairing states. The line for the polar state A_{1u} is shown for comparison. The experimental data are renormalized relative to the upper transition (T_c^+).

ing phase. The results for the low-temperature transport coefficients can shed new light on the strength of the scattering centers because of the sensitivity of the coherence factors to the scattering phase shift. Furthermore, our theoretical results suggest that measurements of the heat transport along different crystal axes can differentiate between the various pairing models that have been proposed for heavy fermion and other unconventional superconductors.

Excellent agreement with experiments on UPt_3 is obtained for pairing states with E_{1g} or E_{2u} symmetry at low temperatures, as well as for the AE-model, whereas no agreement (along the c -axis) could be obtained for the pairing states with B_{1u} and $A_{2u} \oplus iB_{1u}$ symmetries. The differences in the excitation spectrum for E_{1g} and E_{2u} can be observed at very low temperatures, $T \lesssim T^* \sim T_c/12$, when the impurity-induced Andreev band determines the heat conductivity. Measurements of the thermal conductivity ratio, κ_c/κ_b , at very low temperatures ($T \ll T_c$) for various impurity concentrations should further differentiate between these models; the E_{2u} model is predicted to have a universal ratio, while the ratio for the E_{1g} state depends strongly on the concentration and scattering strength of impurities. At high temperatures, $T \sim T_c$, our calculations show deviations from the experimental data, which reflect our neglect of (i) the effect of the onset of superconductivity on the inelastic scattering rate, and (ii) the splitting of the superconducting transition temperature. Finally, we note that our prediction of a universal κ/T at low temperatures is in good agreement with recent experiments on Zn doped $YBa_2Cu_3O_{6.9}$ (Taillefer *et al.* 1997).

Acknowledgments

This work was started at Northwestern University and supported by the National Science Foundation (DMR-9705473), the Science and Technology Center for Superconductivity (DMR 91-20000), the Deutsche Forschungsgemeinschaft, and was completed at Los Alamos National Laboratory under the auspices of the U.S. Department of Energy.

A Linear Response in the Quasiclassical Formulism

A.1 Quasiclassical transport coefficients

The electrical current density is determined by the Keldysh propagator, the Fermi velocity, \mathbf{v}_f , and the density of states per spin, N_f , at the Fermi level,

$$\mathbf{j}_e(\mathbf{R}, t) = 2N_f \int d\mathbf{p}_f \int \frac{d\epsilon}{4\pi i} (e \mathbf{v}_f(\mathbf{p}_f)) \frac{1}{4} \text{Tr} \hat{\tau}_3 \hat{g}^K(\mathbf{p}_f, \mathbf{R}; \epsilon, t), \quad (25)$$

and the heat current density has the form

$$\mathbf{j}_\varepsilon(\mathbf{R}, t) = 2N_f \int d\mathbf{p}_f \int \frac{d\epsilon}{4\pi i} (\epsilon \mathbf{v}_f(\mathbf{p}_f)) \frac{1}{4} \text{Tr} \hat{g}^K(\mathbf{p}_f, \mathbf{R}; \epsilon, t). \quad (26)$$

For weak disturbances from equilibrium the current response is linear in the applied perturbation. Here, we are interested in the electrical and heat current response functions, which define the conductivity tensors by

$$\delta \mathbf{j}_e = \boldsymbol{\sigma} \cdot \mathbf{E}_\omega, \quad \text{and} \quad \delta \mathbf{j}_\varepsilon = -\boldsymbol{\kappa} \cdot \nabla T. \quad (27)$$

We develop the quasiclassical linear response equations for the transport coefficients $\boldsymbol{\kappa}$ and $\boldsymbol{\sigma}$, following the discussion by Rainer and Sauls (1995), and Graf *et al.* (1995).

The advanced, retarded, and Keldysh propagators are calculated from the quasiclassical transport equations

$$[\epsilon \hat{\tau}_3 - \hat{\sigma}_{ext} - \hat{\sigma}^{R,A}, \hat{g}^{R,A}]_\circ = \mathbf{v}_f \cdot \frac{\hbar}{i} \nabla \hat{g}^{R,A}, \quad (28)$$

and

$$\begin{aligned} (\epsilon \hat{\tau}_3 - \hat{\sigma}_{ext} - \hat{\sigma}^R) \circ \hat{g}^K - \hat{g}^K \circ (\epsilon \hat{\tau}_3 - \hat{\sigma}_{ext} - \hat{\sigma}^A) \\ - \hat{\sigma}^K \circ \hat{g}^A + \hat{g}^R \circ \hat{\sigma}^K = \mathbf{v}_f \cdot \frac{\hbar}{i} \nabla \hat{g}^K, \end{aligned} \quad (29)$$

which are supplemented by the normalization conditions (Eilenberger 1968, Larkin & Ovchinnikov 1968),

$$\hat{g}^{R,A} \circ \hat{g}^{R,A} = -\pi^2 \hat{1}, \quad \text{and} \quad \hat{g}^R \circ \hat{g}^K + \hat{g}^K \circ \hat{g}^A = 0. \quad (30)$$

To linear order in the perturbation the quasiparticles (with charge e) respond to an electric field or temperature gradient through the self-energy terms,

$$\hat{\sigma}_{ext} = -\frac{e}{c} \mathbf{v}_f \cdot \mathbf{A} \hat{\tau}_3, \quad \text{or} \quad \mathbf{v}_f \cdot \frac{\hbar}{i} \nabla \hat{g}_0^X, \quad \text{for } X \in \{R, A, K\}, \quad (31)$$

where $\mathbf{A}(\mathbf{q}, \omega)$ is the vector potential describing the transverse field $\mathbf{E}_\omega = (i\omega/c)\mathbf{A}$, and \hat{g}_0^X are the equilibrium propagators. In order to calculate the conductivity we solve the transport equations to linear order in the perturbing fields. For the heat conductivity the perturbation is the temperature gradient ∇T . Generally, deviations arise from *local* equilibrium either from changes in the equilibrium propagators $\nabla \hat{g}_0^{R,A}$ or from the distribution function $\nabla \Phi_0$ with

$$\Phi_0(\mathbf{R}) = 1 - 2f(\epsilon; T(\mathbf{R})) = \tanh\left(\frac{\epsilon}{2k_B T(\mathbf{R})}\right). \quad (32)$$

We consider only spatially homogeneous superconducting states which are in equilibrium, and are “unitary”, i.e., the equilibrium mean-field order parameter satisfies $\hat{\Delta}(\mathbf{p}_f)^2 = -|\Delta(\mathbf{p}_f)|^2 \hat{1}$, where $|\Delta|^2$ stands for either the spin scalar product $\Delta \underline{\Delta}$ or the spin vector product $\underline{\Delta} \cdot \underline{\Delta}$.

A.2 Solutions of the linearized quasiclassical transport equations

The deviations of the propagators from their local equilibrium values, $\delta \hat{g}^X = \hat{g}^X - \hat{g}_0^X$, and $\delta \hat{\sigma}^X = \hat{\sigma}^X - \hat{\sigma}_0^X$ with $X \in \{R, A, K\}$, satisfy the following linearized equations for the retarded and advanced propagators,

$$\left[\delta \hat{g}^{R,A}, \hat{h}^{R,A} \right]_\circ = i\partial \hat{g}_0^{R,A} + \left[\hat{g}_0^{R,A}, \hat{\sigma}_{ext} + \delta \hat{\sigma}^{R,A} \right]_\circ, \quad (33)$$

and for the anomalous propagator,

$$\begin{aligned} \hat{h}^R \circ \delta \hat{g}^a - \delta \hat{g}^a \circ \hat{h}^A &= (i\partial \Phi_0) \circ \hat{g}_0^A - \hat{g}_0^R \circ (i\partial \Phi_0) + \delta \hat{\sigma}^a \circ \hat{g}_0^A - \hat{g}_0^R \circ \delta \hat{\sigma}^a \\ &\quad - [\hat{\sigma}_{ext}, \Phi_0]_\circ \circ \hat{g}_0^A - \hat{g}_0^R \circ [\Phi_0, \hat{\sigma}_{ext}]_\circ, \end{aligned} \quad (34)$$

where $\hat{h}^{R,A} = \epsilon \hat{\tau}_3 - \hat{\sigma}_0^{R,A}$, and $\partial = \hbar \mathbf{v}_f \cdot \nabla$. We introduced Eliashberg’s anomalous propagator, $\delta \hat{g}^a$, and self-energy, $\delta \hat{\sigma}^a$, defined by

$$\delta \hat{g}^K = \delta \hat{g}^R \circ \Phi_0 - \Phi_0 \circ \delta \hat{g}^A + \delta \hat{g}^a, \quad (35)$$

$$\delta \hat{\sigma}^K = \delta \hat{\sigma}^R \circ \Phi_0 - \Phi_0 \circ \delta \hat{\sigma}^A + \delta \hat{\sigma}^a. \quad (36)$$

The transport equations for $\delta \hat{g}^{R,A,a}$ are simplified by inserting the local equilibrium propagators

$$\hat{g}_0^{R,A} = \frac{\tilde{\epsilon}^{R,A} \hat{\tau}_3 - \tilde{\Delta}^{R,A}}{C^{R,A}}, \quad \text{with} \quad C^{R,A} = -\frac{1}{\pi} \sqrt{|\tilde{\Delta}^{R,A}|^2 - (\tilde{\epsilon}^{R,A})^2}, \quad (37)$$

where $\tilde{\epsilon}^{R,A}$ and $\tilde{\Delta}^{R,A}$ determine the equilibrium self-energy,

$$\hat{\sigma}_0^{R,A} = (\epsilon - \tilde{\epsilon}^{R,A}) \hat{\tau}_3 + \tilde{\Delta}^{R,A} + D^{R,A} \hat{1}. \quad (38)$$

Finally, the equations for $\delta\hat{g}^{R,A}$ and $\delta\hat{g}^a$ are solved by using the normalization conditions

$$\hat{g}_0^{R,A} \circ \delta\hat{g}^{R,A} + \delta\hat{g}^{R,A} \circ \hat{g}_0^{R,A} = 0, \quad \text{and} \quad \hat{g}_0^R \circ \delta\hat{g}^a + \delta\hat{g}^a \circ \hat{g}_0^A = 0, \quad (39)$$

and $\hat{h}^{R,A}$ in order to move the propagators $\delta\hat{g}^{R,A}$ and $\delta\hat{g}^a$ to the right on the left hand side of (33) and (34). The solutions are

$$\delta\hat{g}^{R,A} = \left(C_+^{R,A} \hat{g}_0^{R,A} + D_-^{R,A} \right)^{-1} \circ \left(-i\partial\hat{g}_0^{R,A} + [\hat{\sigma}_{ext} + \delta\hat{\sigma}^{R,A}, \hat{g}_0^{R,A}]_\circ \right), \quad (40)$$

$$\begin{aligned} \delta\hat{g}^a = & (C_+^a \hat{g}_0^R + D_-^a)^{-1} \circ \left((i\partial\Phi_0) \circ \hat{g}_0^A - \hat{g}_0^R \circ (i\partial\Phi_0) \right. \\ & \left. + \delta\hat{\sigma}^a \circ \hat{g}_0^A - \hat{g}_0^R \circ \delta\hat{\sigma}^a - [\hat{\sigma}_{ext}, \Phi_0]_\circ \circ \hat{g}_0^A - \hat{g}_0^R \circ [\Phi_0, \hat{\sigma}_{ext}]_\circ \right), \quad (41) \end{aligned}$$

with the auxiliary functions

$$C_+^{R,A}(\mathbf{p}_f; \epsilon, \omega) = C^{R,A}(\mathbf{p}_f; \epsilon_+) + C^{R,A}(\mathbf{p}_f; \epsilon_-), \quad (42)$$

$$D_-^{R,A}(\mathbf{p}_f; \epsilon, \omega) = D^{R,A}(\mathbf{p}_f; \epsilon_+) - D^{R,A}(\mathbf{p}_f; \epsilon_-), \quad (43)$$

$$C_+^a(\mathbf{p}_f; \epsilon, \omega) = C^a(\mathbf{p}_f; \epsilon_+) + C^a(\mathbf{p}_f; \epsilon_-), \quad (44)$$

$$D_-^a(\mathbf{p}_f; \epsilon, \omega) = D^a(\mathbf{p}_f; \epsilon_+) - D^a(\mathbf{p}_f; \epsilon_-), \quad (45)$$

and with $\epsilon_\pm = \epsilon \pm \hbar\omega/2$. Using the normalization conditions (30) we can immediately invert the matrix

$$\left(C \hat{g}_0^{R,A} + D \right)^{-1} = -\frac{C \hat{g}_0^{R,A} - D}{\pi^2 C^2 + D^2}. \quad (46)$$

After combining the previous results (40) and (41), according to (35), we obtain the general expression for the linearized Keldysh propagator $\delta\hat{g}^K$:

$$\begin{aligned} \delta\hat{g}^K = & (C_+^R \hat{g}_0^R + D_-^R)^{-1} \circ \left(-i\partial\hat{g}_0^R + [\hat{\sigma}_{ext} + \delta\hat{\sigma}^R, \hat{g}_0^R]_\circ \right) \circ \Phi_0 \\ & - \Phi_0 \circ (C_+^A \hat{g}_0^A + D_-^A)^{-1} \circ \left(-i\partial\hat{g}_0^A + [\hat{\sigma}_{ext} + \delta\hat{\sigma}^A, \hat{g}_0^A]_\circ \right) \\ & + (C_+^a \hat{g}_0^R + D_-^a)^{-1} \circ \left((i\partial\Phi_0) \circ \hat{g}_0^A - \hat{g}_0^R \circ (i\partial\Phi_0) + \delta\hat{\sigma}^a \circ \hat{g}_0^A - \hat{g}_0^R \circ \delta\hat{\sigma}^a \right. \\ & \left. - [\hat{\sigma}_{ext}, \Phi_0]_\circ \circ \hat{g}_0^A - \hat{g}_0^R \circ [\Phi_0, \hat{\sigma}_{ext}]_\circ \right). \quad (47) \end{aligned}$$

A closer look at (47) shows that changes in the equilibrium propagators $\partial\hat{g}_0^{R,A}$ do not contribute to a static heat current, because the normalization condition (30) gives $2 \text{Tr} \hat{g}_0^{R,A} \partial\hat{g}_0^{R,A} = \partial \text{Tr} (\hat{g}_0^{R,A})^2 = 0$. In linear response the physical observables are then determined by the deviations from the quasiparticle distribution through $\delta\hat{g}^K$. In general the corrections to the self-energies $\delta\hat{\sigma}$ must be included and require a self-consistent calculation.

References

- Present address: Center for Materials Science, Los Alamos National Laboratory, New Mexico 87545.
- Adenwalla S. *et al.* (1990): Phys. Rev. Lett. **65**, 2298
- Arfi B., Bahlouli H., Pethick C. J. (1988): Phys. Rev. Lett. **60**, 2206
- Arfi B., Bahlouli H., Pethick C. J. (1989): Phys. Rev. B **39**, 8959
- Balatsky A. V., Salkola M. L., Rosengreen A. (1995): Phys. Rev. B **51**, 15 547
- Barash Yu. S., Svidzinsky A. A. (1996): JETP Lett., **63**, 296; Phys. Rev. B **53**, 15 254
- Bardeen J., Cooper L. N., Schrieffer J. R. (1957): Phys. Rev. **108**, 1175
- Broholm C. *et al.* (1990): Phys. Rev. Lett. **65**, 2062
- Bruls, G. *et al.*, Phys. Rev. Lett., 65:2294, 1990.
- Buchholtz L. J., Zwicky G. (1981): Phys. Rev. B **23**, 5788
- Chen D. C., Garg A. (1993): Phys. Rev. Lett. **70**, 1689
- Chen D. C., Garg A. (1994): Phys. Rev. B **49**, 479
- Choi C. H., Muzikar P. (1988): Phys. Rev. B **37**, 5947
- Coffey L. , Rice T. M., Ueda K. (1985): J. Phys. C: Solid State Phys. **18**, L813
- Eilenberger G. (1968): Z. Phys. **214**, 195
- Fledderjohann A., Hirschfeld P. J. (1995): Solid State Commun. **94**, 163
- Geilikman B. T. (1958): Zh. Eksp. Teor. Fiz. **34**, 1042; [Sov. Phys. JETP **34**, L721 (1958)]
- Gor'kov L., Kalugin P. (1985): JETP Lett. **41**, 253
- Graf M. J., Palumbo M., Rainer D., Sauls J. A. (1995): Phys. Rev. B **52**, 10 588
- Graf M. J., Yip S.-K., Sauls J. A. (1996a): J. Low Temp. Phys. **102**, 367; (E) **106**, 727
- Graf M. J., Yip S.-K., Sauls J. A., Rainer D. (1996b): Phys. Rev. B **53**, 15 147
- Graf M. J., Yip S.-K., Sauls J. A. (1999): to appear in J. Low. Temp. Phys. **114**; [<http://xxx.lanl.gov/abs/cond-mat/9807370>]
- Heffner R. H., Norman M. R. (1996): Comments Cond. Matt. Phys., **17** 361
- Hirschfeld P. J., Putikka W. O., Scalapino D. J. (1994): Phys. Rev. B **50**, 10 250
- Hirschfeld P. J., Vollhardt D., Wölfle P. (1986): Solid State Commun. **59**, 111
- Hirschfeld P. J., Wölfle P., Einzel D. (1988): Phys. Rev. B **37**, 83
- Hirschfeld P. J. *et al.* (1989): Phys. Rev. B **40**, 6695
- Huxley A. D., Suderow H. , Brison J. P., Flouquet J. (1995): Phys. Lett. A **209**, 365
- Keldysh L. V. (1964): Zh. Eksp. Teor. Fiz. **47**, 1515; [Sov. Phys. JETP **20**, 1018 (1965)]
- Kycia J. B. *et al.* (1998): Phys. Rev. B **58**, 603
- Larkin A. I., Ovchinnikov Yu. N. (1968): Zh. Eksp. Teor. Fiz. **55**, 2262; [Sov. Phys. JETP **28**, 1200 (1969)]
- Lee W., Rainer D., Zimmermann W. (1989): Physica C **159**, 535
- Lussier B., Ellman B., Taillefer L. (1995): Phys. Rev. Lett. **73**, 3294
- Lussier B., Ellman B., Taillefer L. (1996): Phys. Rev. B **53**, 5145
- Machida K., Ozaki M. (1991): Phys. Rev. Lett. **66**, 3293
- Mattis D. C., Bardeen J. (1958): Phys. Rev. **111**, 412
- Monien H., Scharnberg K., Tewordt L., Walker D. (1987): Solid State Commun. **61**, 581
- Müller V. *et al.* (1987): Phys. Rev. Lett. **58**, 1224
- Norman M. R., Hirschfeld P. J. (1996): Phys. Rev. B **53**, 5706
- Ohmi T., Machida K. (1993): Phys. Rev. Lett. **71**, 625
- Pethick C. J., Pines D. (1986): Phys. Rev. Lett. **57**, 118
- Pines D. (1994a): Physica C **235-240**, 113

- Pines D. (1994b): *Physica B* **199-200**, 300
- Preosti G., Kim H., Muzikar P. (1994): *Phys. Rev. B* **50**, 13 638
- Rainer D., Sauls J. A. (1995): In *Superconductivity: From Basic Physics to the Latest Developments*, Lecture Notes of the Spring College in Condensed Matter Physics, I.C.T.P., Trieste, ed. by P.N. Butcher and L. Yu, World Sci., Singapore.
- Rickayzen G. (1976): *Green's Functions and Condensed Matter Physics*. Academic Press, London
- Sauls J. A. (1994a): *Adv. in Phys.* **43**, 113
- Sauls J. A. (1994b): Fermi-liquid theory for unconventional superconductors. In K. S. Bedell, Z. Wang, D. E. Meltzer, V. Balatsky, E. Abrahams, editors, *Strongly Correlated Materials: The Los Alamos Symposium 1993*, page 106, Reading, Mass., Addison Wesley
- Scalapino D. J. (1995): *Physics Report* **250**, 329
- Schmitt-Rink S., Miyake K., Varma C. M. (1986): *Phys. Rev. Lett.* **57**, 2575
- Shivaram B. S., Jeong Y. H., Rosenbaum T. F., Hinks D. G. (1986): *Phys. Rev. Lett.* **56**, 1078
- Signore P. J. C., *et al* (1995): *Phys. Rev. B* **52**, 4446
- Suderow H., Brison J., Huxley A., Flouquet J. (1997): *J. Low Temp. Phys.* **108**, 11
- Sun Y., Maki K. (1995): *Europhys. Lett.* **32**, 355
- Taillefer L., Lonzarich G. (1988): *Phys. Rev. Lett.* **60**, 1570
- Taillefer L. *et al.* (1997): *Phys. Rev. Lett.* **79**, 483
- Volovik G. E., Gor'kov L. P. (1985): *Sov. Phys. JETP* **61**, 843
- Won H., Maki K. (1993): *Phys. Rev. B* **49**, 1397
- Yip S.-K., Sauls J. A. (1992): *J. Low Temp. Phys.* **86**, 257
- Yip S.-K., Garg A. (1993): *Phys. Rev. B* **48**, 3304
- Zhitomirsky M., Ueda K. (1996): *Phys. Rev. B* **53**, 6591